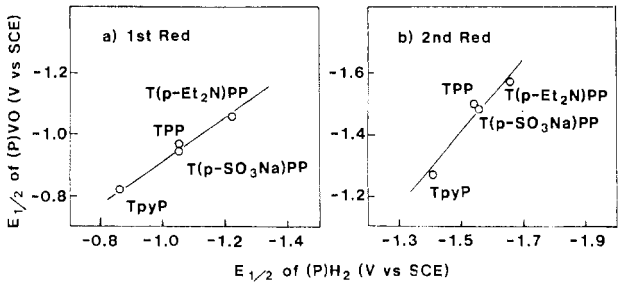

Figure 12. Correlation between half-wave potentials for the first and second reductions of the various vanadyl porphyrins versus half-wave potentials for reduction of the corresponding free-base complex in DMF.

uents affect the reduction potentials. $E_{1/2}$ values for both the first and the second reduction of the vanadyl porphyrins are plotted in Figure 12 against $E_{1/2}$ for the corresponding free-base porphyrin. A good linear relationship is obtained.

Redox potentials for the same series of Ni(II) porphyrins under the same solution conditions have also been measured.[3] Ni(II) has eight electrons in its outer configuration but contains a full complement of d electrons (four) that can interact with the π^* orbitals of the porphyrin. The V(IV) complexes contain only one electron in the d_{xy} orbital and cannot interact with the π^* orbitals of the porphyrin ring.[26]

The results in Figure 12 show that the electronic effect of the porphyrin ring substituents affect the redox potentials of the oxovanadium complexes to a smaller degree than those of the nickel complexes. However, these differences are not large and can be explained by the fact that the empty d_{xz} and d_{yz} orbitals of V(IV) have the proper symmetry for overlap with the filled π orbitals of the porphyrin ring and are lower in energy than the d orbitals of V(IV).

In summary, the porphyrin ring substituents have a strong influence on the redox potentials of both the nickel and the vanadyl complexes. The pyridyl electron-withdrawing substituent in the meso position of the porphyrin ring leads to easier reductions. At the same time the oxidation becomes more difficult.

Acknowledgment. The support of the National Science Foundation (Grant No. CHE-8515411) and the CNRS is gratefully acknowledged.

Registry No. (TpyP)VO, 58593-48-9; [T(*p*-SO_3Na)PP]VO, 93410-57-2; [T(*p*-Et_2N)PP]VO, 114466-58-9; DMF, 68-12-2; Pt, 7440-06-4; CH_2Cl_2, 75-09-2; (TpyP)VO(DMF), 114580-83-5; [T(*p*-SO_3Na)PP]-VO(DMF), 114580-84-6; [(TpyP)VO(DMF)]$^-$, 114594-55-7; [[T(*p*-SO_3Na)PP]VO(DMF)]$^-$, 114614-04-9; [(TpyP)VO]$^{2-}$, 114580-85-7; [[T(*p*-SO_3Na)PP]VO]$^{2-}$, 114580-86-8; [(TpyP)VO]$^-$, 114580-87-9.

(26) Smith, K. M. In *Porphyrins and Metalloporphyrins*; Smith, K. M., Ed.; Elsevier: New York, 1975.

Contribution from the Department of Chemistry, University of Houston, Houston, Texas 77004

Electrochemical Studies of Dimeric Rhodium(III) Porphyrins Containing a Dibasic Nitrogen-Heterocyclic Bridging Ligand

Y. H. Liu, J. E. Anderson, and K. M. Kadish*

Received January 11, 1988

The electrochemistry and spectroelectrochemistry of $[(P)RhCl]_2L$, where P is the dianion of tetraphenylporphyrin (TPP) or octaethylporphyrin (OEP) and L is a conjugated dibasic nitrogen-heterocyclic ligand such as 4,4′-bipyridine (bpy) or *trans*-1,2-bis(4-pyridyl)ethylene (BPE) or a nonconjugated nitrogen-heterocyclic ligand such as 1,2-bis(4-pyridyl)ethane (BPA) or 4,4′-trimethylenebis(pyridine) (TMDP), are reported. The Rh(III) dimers with BPA or TMDP nonconjugated bridging ligands undergo one irreversible metal-centered reduction in tetrahydrofuran or methylene chloride. However, two overlapping irreversible metal center reductions are observed for Rh(III) dimers that are linked via the conjugated bridging ligands, bpy and BPE. In all cases, $[(P)Rh]_2$ and the free nitrogen-heterocyclic ligand are generated as products from one or more chemical reactions that follow the metal-centered reduction of Rh(III) to Rh(II). Two reversible two-electron oxidations are observed for $[(P)RhCl]_2L$, where L = BPE, BPA, and TMDP. This contrasts with the case for $[(P)RhCl]_2$bpy, which undergoes a single reversible two-electron transfer followed by two reversible one-electron oxidations. On the basis of the electrochemical and spectroelectrochemical data, an overall mechanism for reduction and oxidation of the $[(P)RhCl]_2L$ complexes is presented.

Introduction

The electrochemistry of bridged iron porphyrins and iron phthalocyanines of the form $[(P)Fe]_2X$ and $[(Pc)Fe]_2X$, where Pc is the dianion of phthalocyanine, P is the dianion of a given porphyrin macrocycle, and X = C, N, or O, has been reported.[1-7] Multiple single-electron-transfer processes are observed for the above complexes in both the porphyrin and the phthalocyanine series, and this implies an interaction of the two macrocyclic units across the bridging atom. In contrast, replacement of the single-atom bridge in $[(P)Fe]_2X$ with a nitrogen-heterocycle multiatom bridge results in the disappearance of all interactions between the two iron porphyrin units.[8] This is not the case for many non-porphyrin dimeric complexes that are bridged by nitrogen heterocycles. For example, the well-known bridged Ru complexes of the form $[[(NH_3)_5Ru]_2L]^{n+}$, where n = 6, 5 or 4 and L is one of various 4,4′-bipyridyl-type ligands, exhibit extensive interaction between the two metal centers.[9-11] It is thus not clear

(1) Lançon, D.; Kadish, K. M. *Inorg. Chem.* **1984**, *23*, 3942.
(2) Kadish, K. M.; Cheng, J. S.; Cohen, I. A.; Summerville, D. A. In *Electrochemical Studies of Biological Systems*; ACS Symposium Series 38; American Chemical Society: Washington, DC, 1977; Chapter 5.
(3) Kadish, K. M.; Rhodes, R. K.; Bottomley, L. A.; Goff, H. M. *Inorg. Chem.* **1981**, *20*, 3195.
(4) Felton, R. H.; Owen, G. S.; Dolphin, D.; Forman, A.; Borg, D. C.; Fajer, J. *Ann. N.Y. Acad. Sci.* **1973**, *206*, 504.
(5) Chang, D.; Cocolios, P.; Wu, Y. T.; Kadish, K. M. *Inorg. Chem.* **1984**, *23*, 1629.
(6) Bottomley, L. A.; Gorce, J.-N.; Goedken, V. L.; Ercolani, C. *Inorg. Chem.* **1985**, *24*, 3733.
(7) Bottomley, L. A.; Ercolani, C.; Gorce, J.-N.; Pennesi, G. *Inorg. Chem.* **1986**, *25*, 2338.
(8) Gorce, J.-N. Ph.D. Dissertation, Georgia Institute of Technology, 1986.
(9) Creutz, C.; Taube, H. *J. Am. Chem. Soc.* **1969**, *91*, 3988.

0020-1669/88/1327-2320$01.50/0

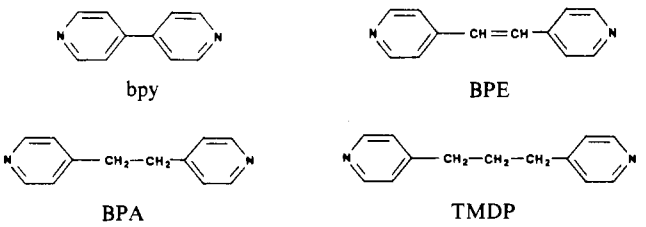

Figure 1. Structures of investigated bridging ligands.

if the lack of any interaction across a bridging nitrogen heterocycle in $[(P)Fe]_2L$ is a general property of all similar bridged metalloporphyrins or is specific to the iron porphyrin complex. It is therefore of interest to examine if interactions will occur for nitrogen-heterocycle-bridged metalloporphyrins with central metals other than iron.

In this paper, we report the electrochemical properties of dibasic nitrogen-heterocycle-bridged rhodium(III) porphyrin complexes of the form $[(P)RhCl]_2L$, where P is the dianion of tetraphenylporphyrin (TPP) or octaethylporphyrin (OEP) and L is 4,4′-bipyridine (bpy), *trans*-1,2-bis(4-pyridyl)ethylene (BPE), 1,2-bis(4-pyridyl)ethane (BPA), or 4,4′-trimethylenebis(pyridine) (TMDP), whose structures are shown in Figure 1.

Experimental Section

Instrumentation and Methods. Cyclic voltammetric measurements were obtained with an IBM EC 225 voltammetric analyzer or an EG&G Princeton Applied Research Model 174A/175 polarographic analyzer/universal programmer coupled with a Houston Instruments Model 2000 X-Y recorder. A Tektronix 5111 storage oscilloscope was used for scan rates higher than 0.5 V/s. A platinum button served as the working electrode and a platinum wire as the counter electrode. A saturated calomel electrode (SCE), which was separated from the bulk solution by a fritted-glass disk, was used as the reference electrode. Bulk controlled-potential coulometry was performed on a EG&G Princeton Applied Research Model 173 potentiostat which contained a Model 179 coulometer system that was coupled with a Princeton Applied Research Model RE-0074 time base X-Y recorder. Thin-layer spectroelectrochemical measurements were made with an IBM EC 225 voltammetric analyzer coupled with a Tracor Northern 1710 spectrometer/multichannel analyzer. Construction of the thin-layer cell is described in the literature.[12] Low-temperature experiments were done by cooling the cell with a dry ice/acetone bath to a constant temperature.

UV–visible spectra were recorded on an IBM 9430 spectrophotometer. ^1H NMR spectra were recorded on either a Nicolet FT-300 or a GE QE-300 spectrometer. The 7.26 ppm peak of the solvent ($CHCl_3$) was used as an internal standard for the ^1H NMR measurements.

Materials. All solvents used for electrochemistry were purified immediately before use. Spectroscopic grade methylene chloride (CH_2Cl_2) was distilled from P_2O_5. Tetrahydrofuran (THF) was distilled from CaH_2 followed by distillation from sodium and benzophenone under nitrogen. Tetra-*n*-butylammonium perchlorate (TBAP) was purchased from Fluka Chemical Co., purified by two recrystallizations from ethyl alcohol, and stored in a vacuum oven at 40 °C. Unless otherwise noted, 0.2 M tetrabutylammonium perchlorate (TBAP) was used as the supporting electrolyte in the electrochemical and spectroelectrochemical measurements.

(TPP)RhCl and (OEP)RhCl were synthesized by the method of Callot[13] and Aoyama et al.,[14] respectively. The bridged rhodium(III) complexes of $[(P)RhCl]_2L$ were prepared according to the method of Thomas.[15] This method involves refluxing 2 equiv of (P)RhCl with 1 equiv of the dibasic N-heterocyclic ligand L. The final products were identified by ^1H NMR and UV–visible spectroscopy.

Results and Discussion

^1H NMR Spectroscopy. Table I summarizes ^1H NMR data for the investigated $[(P)RhCl]_2L$ complexes, and a typical ^1H NMR spectrum of $[(TPP)RhCl]_2TMDP$ is illustrated in Figure 2. The experimental ratio of porphyrin macrocycle to bridging ligand protons in $[(P)RhCl]_2L$ is in agreement with the theoretical ratio for each complex and supports a bridged-dimer formulation in solution.

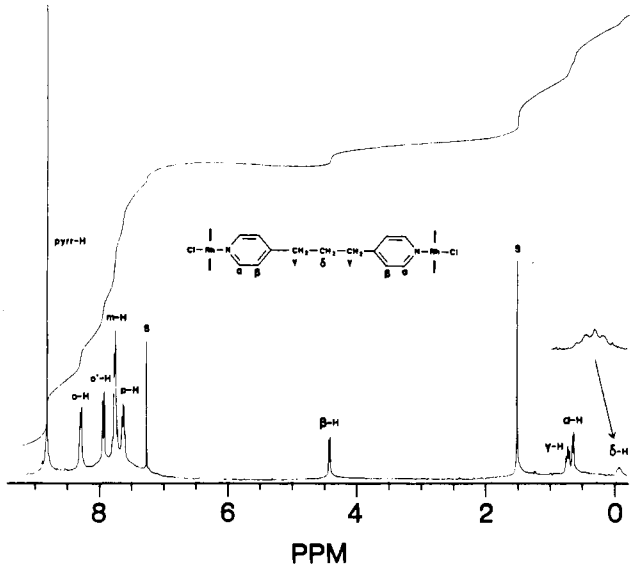

Figure 2. Simplified structure and ^1H NMR spectrum of $[(TPP)RhCl]_2TMDP$ recorded at 17 °C in $CDCl_3$. Solvent peaks are identified by "s".

It is well-known that the oxidation state of the central metal influences the meso proton resonance signals of octaethylporphyrin complexes.[16] Divalent and trivalent metal complexes generally have resonances in the range of 9.75–10.08 and 10.13–10.39 ppm, respectively, but the exact values depend upon the electron-withdrawing or electron-donating ability of any axial ligands that may be complexed with the porphyrin central metal.

The chemical shift of the four meso protons in (OEP)RhCl is located at 10.32 ppm and is comparable to values for other OEP complexes with trivalent central metals. However, there is a deshielding effect from coordination of the bridging ligand (bpy or TMDP) on $[(OEP)RhCl]_2L$, and this results in an upfield shift to 9.95 ppm for $[(OEP)RhCl]_2bpy$ and 10.09 ppm for $[(OEP)RhCl]_2TMDP$. The smaller upfield shift for the latter complex is due to the fact that conjugation between the two pyridines in TMDP is interrupted by a carbon σ-bond. The methylene ($-CH_2CH_3$) and methyl ($-CH_2CH_3$) proton resonances of $[(OEP)RhCl]_2L$ are also affected by the bridging ligand as shown in Table I. Similar electron-donating effects of bound axial ligands on the methylene and methyl protons of OEP complexes are reported in the literature.[17,18]

The resonances of the pyrrole protons in the TPP complexes shift only slightly with changes in the bridging ligand. The splitting of *o*-H and *o*′-H is due to the fact that the bridging ligand of $[(TPP)RhCl]_2L$ produces a nonequivalent environment for the two sets of protons. The *o*-H resonances of $[(TPP)RhCl]_2L$ range between 8.19 and 8.28 ppm while *o*′-H values vary between 7.80 and 7.92 ppm, depending upon the specific L group. Both sets of values may be compared to values of 8.25 (*o*-H) and 8.09 ppm (*o*′-H) for bridged $[(TPP)Rh]_2C_2H_4$.[19]

Normally, *m*-H and *p*-H resonances of tetraphenylporphyrin complexes overlap and cannot be distinguished.[16] However, this is not the case for $[(TPP)RhCl]_2L$, which has separate *m*-H and *p*-H peaks (see Table I and Figure 2). Separate *m*-H and *p*-H resonances have also been reported for $[(TPP)Fe(CS)]_2L$, where L is a dibasic nitrogen heterocycle.[8]

(10) Callahan, R. W.; Brown, G. M.; Meyer, T. J. *Inorg. Chem.* **1974**, *14*, 1443.
(11) Sutton, J. E.; Taube, H. *Inorg. Chem.* **1981**, *10*, 3125.
(12) Lin, X. Q.; Kadish, K. M. *Anal. Chem.* **1985**, *57*, 1498.
(13) Callot, H. J.; Schaeffer, E. *Nouv. J. Chim.* **1980**, *4*, 311.
(14) Aoyama, T.; Yoshida, T.; Sakurai, K.-I.; Ogoshi, H. *Organometallics* **1986**, *5*, 168.
(15) Thomas, N. C. *Transition Met. Chem. (N.Y.)* **1986**, *11*, 425.
(16) Sheer, H.; Katz, J. J. In *Porphyrins and Metalloporphyrins*; Smith, K. M., Ed.; Elsevier: Amsterdam, 1975; Chapter 10.
(17) Yoshida, Z.; Ogoshi, H.; Omura, T.; Watanabe, E.; Kurosaki, T. *Tetrahedron Lett.* **1972**, 1077.
(18) Ogoshi, H.; Omura, T.; Yoshida, Z. *J. Am. Chem. Soc.* **1973**, *95*, 1666.
(19) Wayland, B. B.; Van Voorhees, S. L.; Wilker, C. *Inorg. Chem.* **1986**, *25*, 4039.

Table I. ^{1}H NMR Data for $[(P)RhCl]_2L$, (P)RhCl, and the Free Bridging Ligand L[a,b]

porphyrin, P	bridging ligand, L	protons of P		protons of L[c]	
TPP	bpy	pyr H	8.72 (16 H, s)	α-H	0.59 (4 H, d, 5.97[d])
		o-H	8.19 (8 H, d)	β-H	4.21 (4 H, d, 5.86)
		o'-H	7.80 (8 H, d)		
		m-H	7.69 (16 H, m)		
		p-H	7.57 (8 H, m)		
	BPE	pyr H	8.76 (16 H, s)	α-H	0.72 (4 H, d, 6.25)
		o-H	8.22 (8 H, d)	β-H	4.59 (4 H, d, 6.46)
		o'-H	7.92 (8 H, d)	γ-H	4.92 (2 H, s)
		m-H	7.70 (16 H, m)		
		p-H	7.60 (8 H, m)		
	BPA	pyr H	8.76 (16 H, s)	α-H	0.71 (4 H, d, 6.67)
		o-H	8.23 (8 H, d)	β-H	4.39 (4 H, d, 6.28)
		o'-H	7.91 (8 H, d)	γ-H	0.66 (4 H, s)
		m-H	7.70 (16 H, m)		
		p-H	7.61 (8 H, m)		
	TMDP	pyr H	8.80 (16 H, s)	α-H	0.64 (4 H, d, 6.05)
		o-H	8.28 (8 H, d)	β-H	4.41 (4 H, d, 6.49)
		o'-H	7.92 (9 H, d)	γ-H	0.72 (4 H, t, 7.76)
		m-H	7.75 (16 H, m)	δ-H	−0.08 (2 H, p, 7.79)
		p-H	7.63 (8 H, m)		
(TPP)RhCl		pyr H	8.94 (8 H, s)		
		o-H	8.25 (8 H, m)		
		p-H	7.77 (8 H, m)		
OEP	bpy	meso-H	9.95 (8 H, s)	α-H	−0.24 (4 H, d)
		$-CH_2$	3.89 (32 H, q)	β-H	3.75 (4 H, d)
		$-CH_3$	1.75 (48 H, t)		
	TMDP	meso-H	10.09 (8 H, s)	α-H	−0.08 (4 H, d)
		$-CH_2$	4.02 (32 H, q)	β-H	3.79 (4 H, d)
		$-CH_3$	1.88 (48 H, t)	γ-H	0.47 (4 H, t)
				δ-H	−0.36 (2 H, p)
(OEP)RhCl		meso-H	10.32 (4 H, s)		
		$-CH_2$	4.13 (16 H, m)		
		$-CH_3$	1.98 (24 H, t)		
	bpy[e]			α-H	8.75 (4 H, d, 4.87)
				β-H	7.54 (4 H, d, 5.62)
	BPE[e]			α-H	8.64 (4 H, d, 5.18)
				β-H	7.40 (4 H, d, 5.10)
				γ-H	7.22 (2 H, s)
	BPA[e]			α-H	8.50 (4 H, d, 4.90)
				β-H	7.07 (4 H, d, 4.82)
				γ-H	2.94 (4 H, s)
	TMDP[e]			α-H	8.51 (4 H, d, 4.83)
				β-H	7.10 (4 H, d, 4.87)
				γ-H	2.65 (4 H, t, 7.62)
				δ-H	1.99 (2 H, p, 7.59)

[a] Spectra were recorded at 17 °C in $CDCl_3$. [b] Legend: m = multiplet; p = pentet; q = quartet; t = triplet; d = doublet; s = singlet. [c] α, β, γ, and δ protons of the ligand are identified in Figure 2. [d] J_{H-H} value, in Hz. [e] Uncomplexed nitrogen heterocycle in the absence of the porphyrin.

The α-H and β-H resonances of uncomplexed 4,4'-bipyridine (bpy) are located at 8.75 and 7.54 ppm (see Table I) and differ substantially from those of the bridging 4,4'-bipyridine ligand in $[(OEP)RhCl]_2$bpy and $[(TPP)RhCl]_2$bpy, the latter of which are located at 0.59 (α-H) and 4.21 (β-H) ppm. The 8.16 ppm upfield shift of the bridging ligand α-protons upon formation of $[(TPP)RhCl]_2$bpy is due to shielding by the diamagnetic current from the two porphyrin rings. A similar 6 ppm shift in CH_2 resonances is observed between monomeric $(TPP)Rh(CH_2CH_3)$ (α-H = −4.40 ppm) and bridged $[(TPP)Rh]_2C_2H_4$ (α-H = −10.40 ppm).

The NMR data of the other three $[(P)RhCl]_2L$ complexes are consistent with those of $[(P)RhCl]_2$bpy as well as with NMR data in ref 8 and 15 for similar type complexes. The upfield shift of the bridging ligand proton resonances with respect to that of the same uncomplexed ligand is slightly larger for $[(OEP)RhCl]_2L$ than for $[(TPP)RhCl]_2L$ and is due to the more basic OEP macrocycle. In addition, the large separation in resonances between *o*-H and *o'*-H as well as between *m*-H and *p*-H of $[(TPP)RhCl]_2L$ suggests a very asymmetric structure for this complex.

Reduction of $[(P)RhCl]_2L$. Cyclic voltammograms of the two $[(TPP)RhCl]_2L$ complexes with nonconjugated bridging ligands are depicted in Figure 3a,b. The first reduction (labeled as process I) is irreversible and occurs at $E_p = -1.18$ V for L = TMDP and at $E_p = -1.13$ V for L = BPA. The shape of the current–voltage curve for the first reduction process I is given by $|E_p - E_{p/2}| = 60 \pm 5$ mV and an $i_p/v^{1/2}$ value that is constant. The number of electrons transferred during reduction of $[(TPP)RhCl]_2$TMDP and $[(TPP)RhCl]_2$BPA at −1.40 V in THF was determined by thin-layer coulometry and gave values of $n = 2.3 \pm 0.2$. Both complexes also undergo a second reversible reduction (process II in Figure 3), which occurs at $E_{1/2} = -1.83$ V.

Figure 4a shows the time-resolved electronic absorption spectrum during controlled-potential reduction of $[(TPP)RhCl]_2$TMDP at −1.40 V in THF. The wavelength maxima of the neutral compound shift from initial values of 423, 535, and 570 nm to values of 404 and 496 nm after electroreduction. The final spectrum is characteristic of dimeric $[(TPP)Rh]_2$.[20] This Rh(II) dimer is electroactive and, in THF, can be further reduced at −1.83 V (process II) or oxidized at −0.20 V (process III).[20]

The formation of $[(TPP)Rh]_2$ demonstrates that the reduction of $[(TPP)RhCl]_2L$, where L = BPA and TMDP, is metal-centered. The theory for electron addition to multiple noninteracting redox centers has been presented for reversible electron-transfer reactions.[21] However, the electrochemical data for the irreversible

(20) Kadish, K. M.; Yao, C.-L.; Anderson, J. E.; Cocolios, P. *Inorg. Chem.* **1985**, *24*, 4515.
(21) Flanagan, J. B.; Margel, S.; Bard, A. J.; Anson, F. C. *J. Am. Chem. Soc.* **1978**, *100*, 4248.

Table II. Oxidation and Reduction Potentials (vs SCE) of Dimeric $[(P)RhCl]_2L$ and Monomeric (P)RhCl Complexes in THF and CH_2Cl_2 Containing 0.2 M TBAP

			oxidn,[c] porphyrin ring			redn[c]				
						metal		porphyrin ring	bridging ligand	
complex	solvent	temp, °C	$E_{1/2}$(VI), V	$E_{1/2}$(VII), V	$E_{1/2}$(VIII), V	E_p(Ia), V	E_p(Ib), V	$E_{1/2}$(II), V	$E_{1/2}$(IV), V	E_p(V), V
(TPP)RhCl	THF	23				−1.01				
$[(TPP)RhCl]_2$bpy	THF	23	1.11			−1.02	−1.10	−1.84	−1.86[b]	
		−70	1.10	1.41		−1.15	−1.23	−1.85	−1.86[b]	
	CH_2Cl_2	23	1.02	1.41	1.50	−1.08	−1.14			
		−72	1.04	1.35	1.45	−1.24[a]	−1.24[a]	−1.90	−1.83	
$[(TPP)RhCl]_2$BPE	THF	23	1.08			−1.06	−1.18	−1.85	−1.65	−2.03
		−70	1.07	1.39		−1.20	−1.30	−1.90	−1.63	
	CH_2Cl_2	23	1.01	1.46		−1.06	−1.15			
		−70	1.03	1.41		−1.15	−1.24	−1.89	−1.59	
$[(TPP)RhCl]_2$BPA	THF	23	1.11			−1.13[a]	−1.13[a]	−1.82		
		−70	1.11	1.41		−1.25[a]	−1.25[a]	−1.85		
	CH_2Cl_2	23	1.01	1.44		−1.19[a]	−1.19[a]			
		−70	1.02	1.40		−1.27[a]	−1.27[a]	−1.89		
$[(TPP)RhCl]_2$TMDP	THF	23	1.11			−1.18[a]	−1.18[a]	−1.83		
		−72	1.09	1.37		−1.26[a]	−1.26[a]	−1.85		
	CH_2Cl_2	23	1.01	1.43		−1.19[a]	−1.19[a]			
		−72	1.02	1.43		−1.29[a]	−1.29[a]			
(OEP)RhCl	THF	23	0.95			−1.30				
		−72	0.90	1.28		−1.55		−2.16		
(OEP)RhI	THF	23	0.91			−1.00		−2.14		
		−70	0.89	1.28		−1.36		−2.15		
$[(OEP)RhCl]_2$bpy	THF	23	0.93			−1.18	−1.32		−1.86	
		−70	0.89	1.27		−1.32	−1.48		−1.85	
	CH_2Cl_2	23	0.84	1.30	1.40	−1.34	−1.45			
$[(OEP)RhCl]_2$TMDP	THF	23	0.91			−1.40[a]	−1.40[a]	−2.13		
		−72	0.88			−1.55[a]	−1.55[a]	−2.15		
	CH_2Cl_2	23	0.82	1.34		−1.52[a]	−1.52[a]			

[a] Overlapped two-electron-transfer process (labeled as peak I). [b] Value of $E_{1/2}$ for uncomplexed 4,4′-bipyridine (bpy) in THF containing 0.2 M TBAP. [c] Roman numerals in parentheses correspond to peaks from cyclic voltammograms of $[(P)RhCl]_2L$ complexes in Figures 3 and 5.

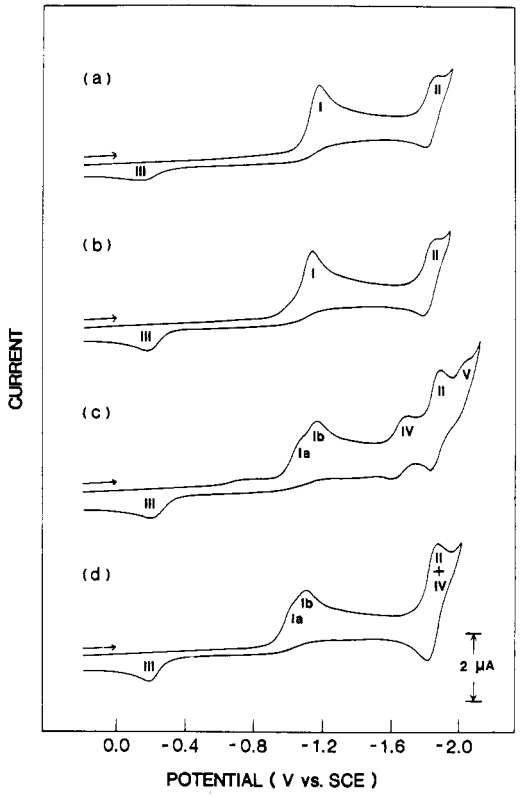

Figure 3. Cyclic voltammograms of (a) $[(TPP)RhCl]_2$TMDP, (b) $[(TPP)RhCl]_2$BPA, (c) $[(TPP)RhCl]_2$BPE, and (d) $[(TPP)RhCl]_2$bpy in THF, 0.2 M TBAP (scan rate 0.1 V/s).

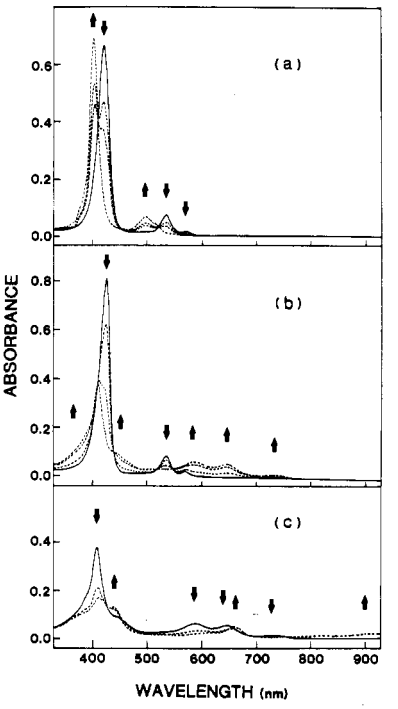

Figure 4. Time-resolved electronic absorption spectra of $[(TPP)RhCl]_2$TMDP: (a) in THF, 0.2 M TBAP at an applied potential of −1.40 V; (b) in CH_2Cl_2, 0.2 M TBAP at an applied potential of +1.20 V; (c) in CH_2Cl_2, 0.2 M TBAP at an applied potential of +1.60 V.

reactions in Figure 3a,b also suggest that the two Rh(III) centers are noninteracting. The reduction potentials of $E_p = -1.13$ V for $[(TPP)RhCl]_2$BPA and $E_p = -1.18$ V for $[(TPP)RhCl]_2$TMDP are very close to $E_p = -1.18$ V for reduction of monomeric (TPP)Rh(L)Cl, where L = dimethylamine, under the same solution conditions.[20] An almost identical result is obtained for reduction of $[(OEP)RhCl]_2$TMDP. The two-electron reduction of this complex also seems to occur at two noninteracting Rh(III) centers and is followed by a chemical reaction to generate dimeric $[(OEP)Rh]_2$.

In contrast to the case for $[(P)RhCl]_2$TMDP and $[(P)RhCl]_2$BPA, the $[(P)RhCl]_2L$ complexes with conjugated bridging ligands show two separate irreversible reductions. This is illustrated in Figure 3c,d, where the two reductions of $[(TPP)RhCl]_2$BPE and $[(TPP)RhCl]_2$bpy are labeled as processes Ia and

Scheme I

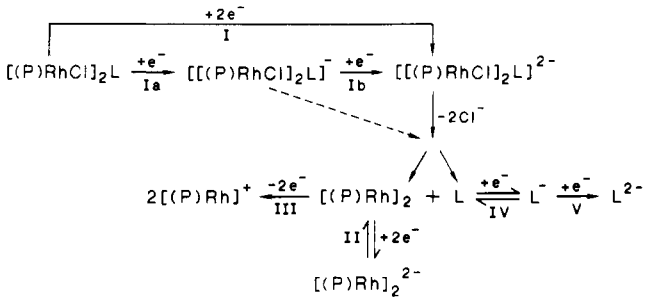

Ib. Two irreversible reductions are also found for $[(OEP)RhCl]_2bpy$ at $E_p = -1.18$ and -1.32 V in THF, 0.2 M TBAP. These peak potentials, as well as those for other processes of the investigated complexes and monomeric (P)RhX, where X = Cl^- or I^-, are given in Table II.

Processes Ia and Ib are due to the successive addition of one electron to $[(P)RhCl]_2L$ and $[[(P)RhCl]_2L]^-$, where L is one of the two conjugated bridging ligands, bpy or BPE. This was ascertained by utilizing tetrabutylammonium chloride ((TBA)Cl) as the supporting electrolyte in THF. Under these experimental conditions, $[(TPP)RhCl]_2bpy$ still undergoes two consecutive irreversible reductions. This rules out the possibility that processes Ia and Ib are due to the mixture of species such as $[(TPP)Rh(ClO_4)]_2L$, $ClO_4^-(TPP)Rh^+$–L–Rh(TPP)Cl, and $[(TPP)RhCl]_2L$, which would result from a dissociation of one or both Cl^- ions from $[(TPP)RhCl]_2L$.

The ^1H NMR spectrum of $[(TPP)RhCl]_2bpy$ was also measured in an $AgClO_4$-saturated $CDCl_3$ solution. Neither monomeric (TPP)RhCl(L) nor free ligand, L, was detected in the ^1H NMR spectrum, and $[(TPP)RhCl]_2L$ was the only species in solution under the investigated experimental conditions. Thus, the two irreversible reductions of $[(TPP)RhCl]_2BPE$, $[(TPP)RhCl]_2bpy$, and $[(OEP)Rh]_2bpy$ are attributed to a stepwise reduction of the two Rh(III) metals in the bridged dimer. This implies that a change from a nonconjugated to a conjugated ligand in $[(P)RhCl]_2L$ results in a change from a noninteracting to an interacting system.

The products after controlled-potential reduction of $[(TPP)RhCl]_2BPE$ or $[(TPP)RhCl]_2bpy$ in THF are $[(TPP)Rh]_2$ and uncomplexed heterocyclic ligand, both of which can undergo further reductions within the potential range of THF. The bpy and BPE nitrogen heterocycles have the same reduction potentials when they are not in the presence of porphyrin species as when they are liberated from $[(P)RhCl]_2L$. These reductions occur at $E_{1/2} = -1.86$ V for L = bpy and at $E_{1/2} = -1.65$ V and $E_p = -2.03$ V for L = BPE. No reductions of BPA or TMDP occur within the negative potential range of THF. Thus, the overall mechanism for reduction of $[(TPP)RhCl]_2L$ in THF is proposed to occur as shown in Scheme I.

An attempt was made to spectrally characterize the mixed-valent singly reduced $[[(TPP)RhCl]_2L]^-$. However, a fast chemical reaction follows the initial electron transfer and this transient anionic species could not be monitored by spectroelectrochemistry, which only showed the ultimate formation of dimer. ESR measurements of the reduced solution did not show any signals corresponding to $[[(TPP)RhCl]_2L]^-$, and low-temperature electrochemical studies gave essentially the same behavior as observed at room temperature.

Oxidation of $[(P)RhCl]_2L$. The $[(OEP)RhCl]_2L$ and $[(TP-P)RhCl]_2L$ complexes with L = BPE, BPA, and TMDP are oxidized in two reversible steps, which are labelled as processes VI and VII. This is shown in Figure 5a for the case of $[(TPP)RhCl]_2TMDP$. In contrast, $[(TPP)RhCl]_2bpy$ and $[(OEP)RhCl]_2bpy$ undergo three reversible oxidations in CH_2Cl_2, 0.2 M TBAP. These oxidations are labeled as processes VI–VIII and are illustrated for the case of $[(TPP)RhCl]_2bpy$ in Figure 5b. Process VI for $[(TPP)RhCl]_2TMDP$ and $[(TPP)RhCl]_2bpy$ has $|E_p - E_{p/2}| = 60 \pm 5$ mV and a constant value of $i_p/v^{1/2}$. Controlled-potential bulk coulometry at +1.10 V gives a coulometric

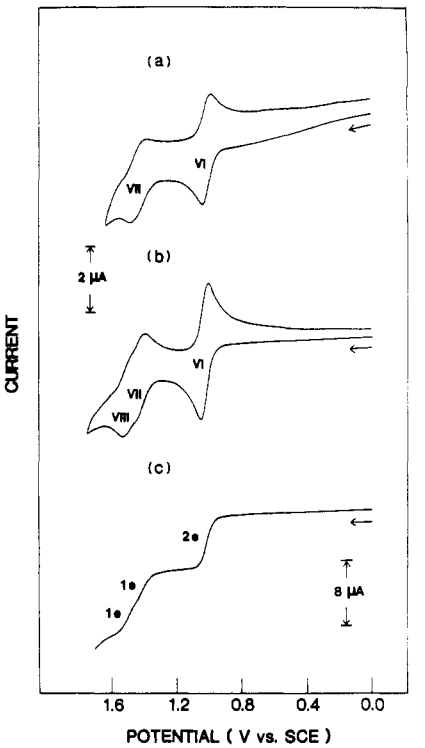

Figure 5. Cyclic voltammograms of (a) $[(TPP)RhCl]_2TMDP$ and (b) $[(TPP)RhCl]_2bpy$ in CH_2Cl_2, 0.2 M TBAP (scan rate 0.1 V/s). Normal pulse voltammogram of (c) $[(TPP)RhCl]_2bpy$ under the same solution conditions.

Scheme II

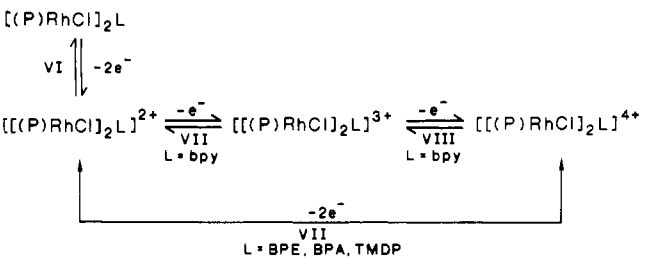

value of $n = 2.0 \pm 0.1$, thus suggesting two noninteracting sites in the overall two-electron-transfer reaction.

Spectral monitoring of the oxidation products show that a porphyrin cation radical is formed during controlled-potential electrolysis of $[(TPP)RhCl]_2TMDP$ in CH_2Cl_2 at +1.20 V. These spectral changes are shown in Figure 4b. The time-resolved UV–visible spectrum obtained after the second oxidation of $[(TPP)RhCl]_2TMDP$ in CH_2Cl_2 is shown in Figure 4c and clearly demonstrates the formation of a porphyrin π dication. However, it should be noted that characteristic π dication absorptions between 800 and 900 nm are not observed for oxidized monomeric Rh(III) porphyrin complexes of the type (P)Rh(L)Cl and (P)-$Rh(L)_2^+Cl^-$, where L = dimethylamine.[22] The spectra in Figure 4c were obtained at times between 0 and 30 s after the controlled-potential electrolysis was initiated. At longer electrolysis times, these absorptions decreased as an absorption at 660 nm increased in intensity.

The half-wave potentials for process VI range between 1.01 and 1.11 V, depending upon the solvent and the temperature (see Table II), and are very close to $E_{1/2} = 0.98$ V for the first oxidation of monomeric (TPP)Rh(L)Cl, where L = dimethylamine, in CH_2Cl_2.[22] Similar to the case for $[(P)RhCl]_2L$, the initial oxidation of (TPP)Rh(L)Cl is reversible and is porphyrin ring centered.

The second and the third reversible oxidations of $[(TPP)RhCl]_2bpy$ and $[(OEP)RhCl]_2bpy$ (processes VII and VIII) in-

(22) Yao, C.-L. Ph.D. Dissertation, University of Houston, 1987.

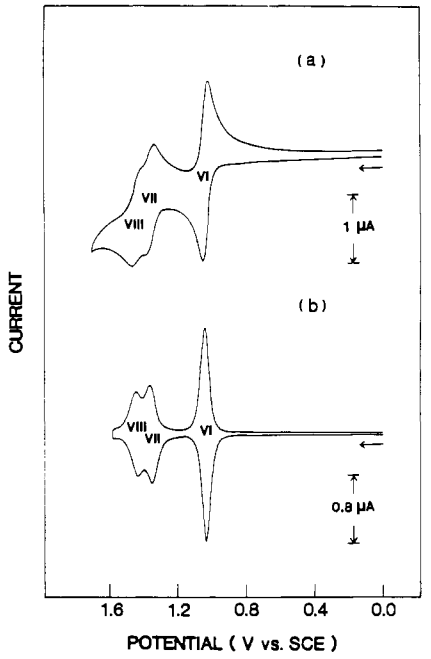

Figure 6. (a) Cyclic voltammogram and (b) differential pulse voltammogram of $[(TPP)RhCl]_2bpy$ in CH_2Cl_2, 0.2 M TBAP at −72 °C.

volve two overlapping one-electron-transfer processes. A normal pulse voltammogram of $[(TPP)RhCl]_2bpy$ is depicted in Figure 5c and shows the number of electrons involved in each oxidation step to be two, one, and one. All of these reversible oxidations involve the intact Rh(III) dimer and not decomposition products from the original material. This is also demonstrated by the cyclic voltammogram for oxidation of $[(TPP)RhCl]_2bpy$ in CH_2Cl_2 at −72 °C. This voltammogram is shown in Figure 6a and is similar to the voltammogram obtained at room temperature.

The differential pulse voltammogram of $[(TPP)RhCl]_2bpy$ at −72 °C (Figure 6b) also demonstrates the reversibility of each electron-transfer process. The data indicate that the two porphyrin rings of $[(TPP)RhCl]_2bpy$ are equivalent, but this is not the case for $[[(TPP)RhCl]_2bpy]^{2+}$, which shows an interaction across the bridging nitrogen heterocycle. Similar behavior was not found for the other three bridging-ligand systems, and an overall oxidation mechanism of $[(P)RhCl]_2L$ is shown in Scheme II.

In summary, the data in this study indicate that the presence of a bridging ligand between two rhodium porphyrin units does not substantially alter the electrochemical behavior of the individual rhodium(III) complexes. The initial reductions of $[(P)RhCl]_2L$ are all metal-centered and are followed by a rapid chemical reaction that leads to a Rh(II) monomer and the ultimate formation of $[(P)Rh]_2$ in THF. The oxidations are all porphyrin ring centered and lead to π cation radicals. However, this study does clearly demonstrate that an interaction between two bridged porpyrin units is possible for complexes that contain a nitrogen-heterocycle bridging ligand and a porphyrin central metal other than iron.

In principle, the reduction of $[(P)RhCl]_2L$, where L = bpy or BPE, generates a short-lived mixed-valence complex. If one assumes that reduction process Ib is due to the intact dimer, an equilibrium constant for formation of the mixed-valence state can be calculated. However, process Ib may be due to the reduction of monomeric (P)RhCl(L) formed by decomposition of the monoanion, $[[(P)RhCl]_2L]^-$. A distinction between the two cases is only possible if the monoanion can be stabilized. This is not the case for the present series of compounds.

Acknowledgment. The support of the National Science Foundation (Grant CHE-8515411) is gratefully acknowledged.

Registry No. bpy, 553-26-4; BPE, 13362-78-2; BPA, 4916-57-8; TMDP, 17252-51-6; $[(TPP)RhCl]_2bpy$, 114550-19-5; $[(TPP)RhCl]_2BPE$, 114533-28-7; $[(TPP)RhCl]_2BPA$, 114533-29-8; $[(TPP)RhCl]_2TMDP$, 114533-30-1; $[(OEP)RhCl]_2bpy$, 106468-35-3; $[(OEP)RhCl]_2BPE$, 114550-16-2; $[(OEP)RhCl]_2BPA$, 114550-17-3; $[(OEP)RhCl]_2TMDP$, 114550-18-4; $[(TPP)Rh]_2$, 88083-37-8; $[(OEP)Rh]_2$, 63439-10-1; (TPP)RhCl, 77944-60-6; (OEP)RhCl, 36670-30-1; (OEP)RhI, 69509-36-0; THF, 109-99-9; Rh, 7440-16-6; Pt, 7440-06-4; CH_2Cl_2, 75-09-2.

Contribution from the Departments of Chemistry, Georgetown University, Washington, D.C. 20057, and Obafemi Awolowo University, Ile-Ife, Nigeria

Nonbridging Ligand Effects as Mechanistic Probes in Ruthenium(III)–Titanium(III) Electron-Transfer Reactions

Kejian Lu,[†] J. Folorunso Ojo,*[,‡] and Joseph E. Earley*[,†]

Received February 3, 1987

Rates of reduction of $Ru(NH_3)_5(pyridine)^{3+}$ by Ti(III) complexes of pentanedione (at 25.0 °C and 1.0 M LiCl) are as predicted from redox potentials of the complexes and the rate–potential relationship followed by Ru(III)–Ti(III) reactions that involve outer-sphere mechanisms. Intermediates, corresponding to an inner-sphere mechanism, are observed for reductions of $Ru_2(CH_3COO)_2(C_2O_4)_2^-$ by Ti^{3+} and by $TiC_2O_4^+$. No intermediate is observable for the reaction of $Ti(C_2O_4)_2^-$ with that oxidant, but the rate indicates an inner-sphere mechanism for the reaction. Nonbridging oxalate ligands on Ti(III) reduce the stability of the intermediate. The rate of electron transfer within the intermediate is significantly increased by the second oxalate added. Stability constants (at 25.0 °C and 1.0 M LiCl) for $TiC_2O_4^+$ and $Ti(C_2O_4)_2^-$ were found to be 8.5×10^5 M^{-1} and 2.5×10^5 M^{-1}.

The rate constant for reduction of $Ru(NH_3)_5py^{3+}$ by $Ti(OH)^{2+}$ falls on a linear free energy relationship (between redox rate constant and reaction free energy) along with rate constants for other Ru(III)–Ti(III) reactions that follow outer-sphere electron-transfer (hereafter ET) mechanisms.[1] Rate constants[2] for Ti(III) reduction of both $Ru(NH_3)_4C_2O_4^+$ and $Ru(NH_3)_5C_2O_4^+$ are 10^4 faster than expected on the basis of that linear free energy relationship. The reductant attacks at the carbonyl oxygen adjacent to the metal atom. ET through structure I is rapid. In

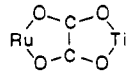

I

contrast, the redox reaction between $Ru_2(CH_3COO)_2(C_2O_4)_2^-$ and Ti(III) occurs by an inner-sphere mechanism with attack of the reductant at a remote, uncomplexed carboxylic group, but an

[†] Georgetown University.
[‡] Obafemi Awolowo University.

(1) Davis, K. M.; Earley, J. E. *Inorg. Chem.* **1978**, *17*, 3350.
(2) Adegite, A.; Earley, J. E.; Ojo, J. F. *Inorg. Chem.* **1979**, *18*, 1535.

0020-1669/88/1327-2325$01.50/0